PCCP

ROYAL SOCIETY OF CHEMISTRY

PAPER

View Article Online
View Journal | View Issue

Cite this: *Phys. Chem. Chem. Phys.*, 2021, **23**, 9337

Correlating Bromelain's activity with its structure and active-site dynamics and the medium's physical properties in a hydrated deep eutectic solvent†

Nilimesh Das, Tanmoy Khan, Navin Subba and Pratik Sen *

Deep eutectic solvents (DESs) are emerging as new media of choice for biocatalysis due to their environmentally friendly nature, fine-tunability, and potential biocompatibility. This work deciphers the behaviour of bromelain in a ternary DES composed of acetamide, urea, and sorbitol at mole fractions of 0.5, 0.3, and 0.2, respectively (0.5Ac/0.3Ur/0.2Sor), with various degrees of hydration. Bromelain is an essential industrial proteolytic enzyme, and the chosen DES is non-ionic and liquid at room temperature. This provides us with a unique opportunity to contemplate protein behaviour in a non-ionic DES for the very first time. Our results infer that at a low DES concentration (up to 30% V/V DES), bromelain adopts a more compact structural conformation, whereas at higher DES concentrations, it becomes somewhat elongated. The microsecond conformational fluctuation time around the active site of bromelain gradually increases with increasing DES concentration, especially beyond 30% V/V. Interestingly, bromelain retains most of its enzymatic activity in the DES, and at some concentrations, the activity is even higher compared with its native state. Furthermore, we correlate the activity of bromelain with its structure, its active-site dynamics, and the physical properties of the medium. Our results demonstrate that the compact structural conformation and flexibility of the active site of bromelain favour its proteolytic activity. Similarly, a medium with increased polarity and decreased viscosity is favourable for its activity. The presented physical insights into how enzymatic activity depends on the protein structure and dynamics and the physical properties of the medium might provide useful guidelines for the rational design of DESs as biocatalytic media.

Received 5th January 2021,
Accepted 24th March 2021

DOI: 10.1039/d1cp00046b

rsc.li/pccp

1. Introduction

Obtaining environmentally safer solvents has always been at the heart of green chemistry.[1–8] Ionic liquids (ILs) are the most studied solvents in this regard and they appear to be environmentally friendly, non-volatile, and highly stable, and can dissolve a broad spectrum of solutes.[9,10] Moreover, one can tune the physical properties of ILs systematically *via* changing the cations and anions.[11,12] Recently, deep eutectic solvents (DESs) have emerged as a new class of solvent,[13] maintaining all the properties of IL.[14] Additionally, the preparation of DESs is more straightforward (only through mixing and heating) and is also cost-effective. The properties of DESs can be fine-tuned not only *via* changing the constituents (as in the case of ILs) but also *via* changing their mole fractions.[15,16] Moreover, many components from natural sources are used to prepare DESs. Such DESs are called natural deep eutectic solvents (NADESs) and are supposed to be much less toxic than ILs.[17–19] Proteins are generally stable only in aqueous solutions. Perhaps, if one can stabilize a protein in some alternate medium where it can carry out its function, it will open up new areas in the field of biocatalysis. Therefore, many studies have been carried out to investigate the structures and activities of proteins in ILs,[20,21] and in the last 2-3 years, DESs have been explored as a potential medium in which protein structure/activity can be retained or even refolded/increased.[22–36] Further, DESs also serve as matrices where proteins remain active under extreme conditions.[37–39]

Enzymes are vital entities for cell function and, moreover, there has been significant interest in the use of structurally

Department of Chemistry, Indian Institute of Technology Kanpur, Kanpur – 208 016, UP, India. E-mail: psen@iitk.ac.in; Fax: +91-51-2259-6806; Tel: +91-51-2259-7436

† Electronic supplementary information (ESI) available: The secondary structural parameters of untagged, CPM-tagged, and TMR-tagged bromelain; CD spectra and secondary structural parameters of native bromelain and back-extracted bromelain from various DES compositions; the absorption spectra of free CPM, CPM tagged to bromelain, free TMR, and TMR-tagged bromelain; fitting comparisons of the fluorescence autocorrelation traces of CPM, CPM tagged to bromelain, TMR, and TMR tagged to bromelain; normalized fluorescence intensity autocorrelation curves for rhodamine 6G at some representative DES concentrations; variations of viscosity with increasing DES concentration; and autocorrelation traces of CPM tagged to bromelain at different laser powers. See DOI: 10.1039/d1cp00046b

stable and active enzymes in industrial processes.[40–42] Bromelain is an industrially important plant-based cysteine protease obtained from pineapple stems.[43] Traditionally it is used in meat tenderizing and protein cleavage.[44] It is also used as a medicine to treat inflammation, thrombosis, arthritis, and so forth.[45,46] The structure, stability, and activity of bromelain have previously been investigated in the presence of several external perturbation sources, including osmolytes, denaturants, and macromolecular crowders.[47–54] However, like any other enzyme, the use of harsh organic solvents might destroy the stability and activity of bromelain and limit its use. On the other hand, Kumar *et al.* showed that the stability and activity of bromelain can be preserved in the presence of a choline-based IL.[55] Similarly, the Venkatesu group showed that the stability and activity of bromelain increase at lower imidazolium-based IL levels and at higher content levels, the activity decreases.[56,57]

However, there are many gaps in the study of bromelain (and enzymes in general) in alternate media. Firstly, there are no studies on the structure and activity of bromelain in DESs. Secondly, enzymes are dynamic entities, and the associated dynamics on the μs timescale are very important for their activities.[58,59] Recently, there have been some attempts to contemplate the μs dynamics in ILs.[60–66] However, to the best of our knowledge, no studies have been conducted to reveal the μs protein dynamics in DESs. Thirdly, most DESs are ionic and the few studies that have been carried out to understand protein behaviour in DESs have been done in such ionic DESs.[26–36] Most non-ionic interactions are weaker than ionic interactions, so non-ionic DESs are challenging to form. However, from an applications point of view when using these DESs as solvents, which demands good solubility, many solutes (like hydrophobic ones) may not dissolve in ionic DESs. Non-ionic DESs can overcome this problem. Therefore, understanding protein behaviour in non-ionic DESs is important. However, there have been no reports to date. Fourthly, there is little understanding of why proteins are stable and retain their activities in DESs.

In this direction, we aim to explore the structural, functional, and dynamic responses of bromelain in a ternary DES composed of acetamide, urea, and sorbitol, with mole fractions of 0.5, 0.3, and 0.2, respectively (0.5Ac/0.3Ur/0.2Sor),[67] with various degrees of hydration. The purposefully chosen DES is non-ionic and a liquid at room temperature. We also attempted to decipher the correlations between these responses. Further, the correlations between the activity of bromelain and the DES properties (*e.g.*, the extent of hydration, viscosity, and polarity) have been explored. The present work might give physical insight into the rational design of DESs.

2. Experimental

2.1. Materials

Bromelain (Fig. 1), casein, 7-diethylamino-3-(4-maleimidophenyl)-4-methylcoumarin (CPM), and tetramethylrhodamine-5-maleimide (TMR) were all purchased from Sigma-Aldrich and used as received. Analytical grade disodium hydrogen phosphate and sodium dihydrogen phosphate were purchased from Merck, India, and were used to prepare buffer solutions (pH 7.4). Dialysis membrane tubing (12 kDa cut-off) was purchased from Sigma-Aldrich and it was washed according to the procedure given by Sigma-Aldrich. A centrifugal filtration unit (Amicon Ultra, 10 kDa cut-off) was purchased from Merck Millipore, Germany. HPLC-grade dimethyl sulfoxide (DMSO) was purchased from S. D. Fine Chemicals Limited, India, and used after distillation. We purchased acetamide from Fisher Scientific and urea from Sigma-Aldrich, dried them under vacuum, and used them without any further purification. Sorbitol was purchased from SD Fine Chemicals Ltd, India, and was dried overnight under vacuum before use.

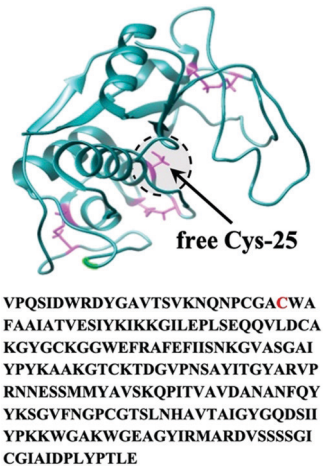

Fig. 1 The amino acid sequence and 3D structure of bromelain (PDB ID: 1W0Q). The single free cysteine residue (Cys-25) is highlighted.

2.2. Protein labelling

We followed the standard procedure of thiol chemistry for protein labelling. Both CPM and TMR have previously been tagged site-specifically to the free thiol group of bromelain, and we follow a similar technique (see Fig. 2a and c).[60,68,69] Briefly, 192 mg of bromelain was dissolved in 19 ml of phosphate buffer (50 mM, pH 7.4). 3.2/3.8 mg of CPM/TMR dissolved in 1 ml of DMSO was added dropwise to the protein solution under continuous stirring. The reaction mixture was then kept at 20 °C under stirring conditions for 12 h, followed by dialysis at 5 °C using 1000 ml of 15 : 1 (V/V) phosphate buffer (50 mM, pH 7.4) and DMSO. The dialysis medium was changed every 12 h for 4 days and after that dialysis was carried out with buffer until the dialyzed solution showed no appreciable fluorescence. The CPM/TMR-tagged bromelain was then concentrated using the 10 kDa-cut-off centrifugal filtration unit. The tagging efficiency is calculated from the ratio of the concentration of bromelain to dye in the CPM/TMR-tagged bromelain, using $\varepsilon^{280}_{\text{bromelain}}$, $\varepsilon^{390}_{\text{CPM}}$, and $\varepsilon^{555}_{\text{TMR}}$ values of 63 500 M^{-1} cm^{-1}, 33 000 M^{-1} cm^{-1}, and 75 000 M^{-1} cm^{-1}, respectively.[68–70]

2.3. Preparation and characterisation of the 0.5 acetamide + 0.3 urea + 0.2 sorbitol (0.5Ac/0.3Ur/0.2Sor) DES

Acetamide and urea form a DES with a eutectic temperature of 318 K at Ac : Ur = 0.6 : 0.4. Recently we showed that the presence

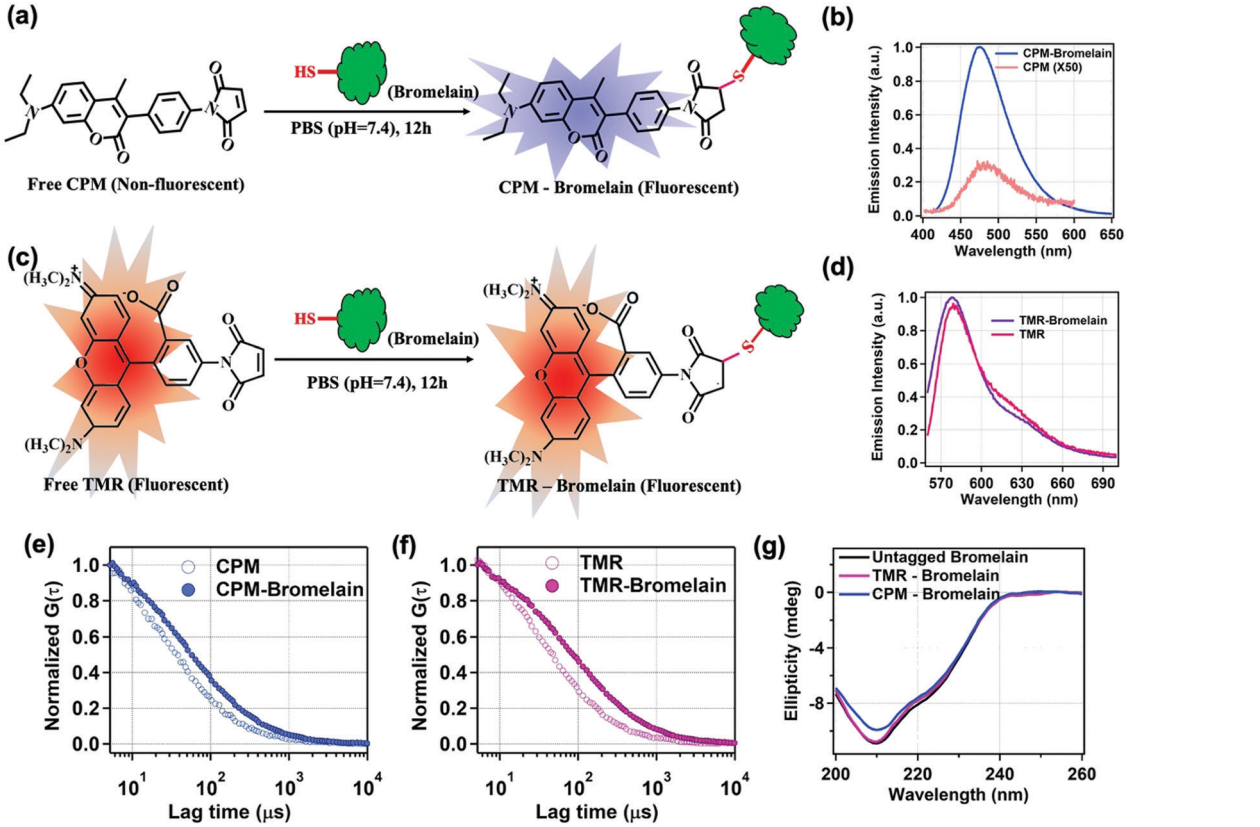

Fig. 2 The tagging of bromelain. (a) A site-specific bromelain tagging scheme with CPM. (b) The emission spectra of CPM (orange) and CPM tagged to Cys-25 of bromelain (blue). The emission spectrum of untagged CPM has been multiplied by a factor of 50 to make it visible. (c) A site-specific bromelain tagging scheme with TMR. (d) The emission spectra of TMR (pink) and TMR tagged to Cys-25 of bromelain (purple). (e) Normalised fluorescence intensity autocorrelation traces for CPM (open blue circles) and CPM tagged to bromelain (filled blue circles). (f) Normalised fluorescence intensity autocorrelation traces for TMR (open pink circles) and TMR tagged to bromelain (filled pink circles). (g) CD spectra of untagged bromelain (black), TMR-tagged bromelain (pink), and CPM-tagged bromelain (blue).

of sorbitol in the acetamide/urea DES system lowered the freezing point of the DES to a large extent, and we reported the complete phase diagram of the ternary system.[67] In this study, we chose a particular ternary Ac/Ur/Sor DES composition with mole fractions of 0.5 acetamide + 0.3 urea + 0.2 sorbitol. The DES is prepared *via* simply mixing the required amounts of acetamide, urea, and sorbitol in an air-tight round-bottom flask, while heating at 343–353 K, until a homogeneous liquid was obtained. Although the exact freezing point cannot be measured, the resulting DES is liquid even at 280 K. The density of our DES system is 1.2521 g mL^{-1} at 303 K.

2.4. Sample preparation

For all the experiments, we used 50 mM pH 7.4 phosphate buffer. The samples are equilibrated overnight. The concentration of bromelain is measured using its molar absorption coefficient of 63 500 M^{-1} cm^{-1} at 280 nm.[70] We used untagged bromelain for activity measurements, CPM-tagged bromelain for steady-state emission studies, and TMR-tagged bromelain for FCS studies. The bromelain concentration is kept at ~10 μM for CD measurements, ~4 μM for steady-state emission experiments, and ~5 nM for FCS measurements. Due to the high absorbance of the DES, CD data of bromelain with the DES could not be recorded. We back-extracted bromelain from the DES, dissolved it in buffer, and recorded the CD spectrum. For back extraction, overnight-equilibrated samples are taken in a centrifugal filtration unit (Amicon Ultra, 10 kDa cut-off) and washed with buffer several times.

2.5. Instrumentation and analysis

2.5.1. CD spectroscopy. We recorded circular dichroism spectra using a commercial CD spectrometer (J-815, Jasco, Japan) using a 2 mm-pathlength cuvette. We analyzed our CD data using CDNN software (http://gerald-boehm.de).[71]

2.5.2. Steady-state absorption and emission spectra. We recorded steady-state absorption and emission spectra using a commercial double-beam spectrophotometer (UV-2450, Shimadzu, Japan) and spectrofluorimeter (FluoroMax-4, Jobin-Yvon, USA), respectively, using a 10 mm-pathlength cuvette.

2.5.3. Fluorescence correlation spectroscopy (FCS). We performed fluorescence correlation spectroscopic (FCS) measurements using an instrument built in our laboratory, the details of which can be found in our previous publications.[69,72–75] We used an inverted microscope (IX-71, Olympus, Japan) with a 60 × 1.2 NA water-immersion objective (UplanSApo, Olympus, Japan) in this setup. The sample was kept on a cover slip

(Blue Star, Polar Industrial Corporation, India) on the microscope sample platform. Depending on the fluorophore, either a 405 nm (MDL-III-405-5mW, China) or a 532 nm (MGL-III-532-5mW, China) laser source was used to create a confocal observation volume 40 μm above the upper surface of the cover slip. The emitted photons, collected using the same objective, travel through a dichroic mirror (ZT405rdc, Chroma Tech. Corp., USA, for 405 nm excitation and ZT532rdc, Chroma Tech. Corp., USA, for 532 nm excitation), emission filter (FSQ-GG455, Newport, USA, for 405 nm excitation and 605/70 m, Chroma Tech. Corp., USA), and multimode fiber patch chord (M67L01 25μm 0.10NA, ThorLabs, USA) before reaching the detector (SPCM-AQRH-13-FC, Excelitas Tech. Inc., Canada). The detected photons were autocorrelated using a correlator card (FLEX990EM-12E, correlator.com, USA) and displayed using the LabVIEW® program on a computer. For a single component system, assuming a Gaussian detection volume, the autocorrelation function can be written as follows:[76]

$$G(\tau) = \frac{1}{N}\left(1+\frac{\tau}{\tau_D}\right)^{-1}\left(1+\frac{\tau}{\omega^2\tau_D}\right)^{-1/2} \quad (1)$$

$$G(\tau) = \frac{1}{N}\left(1+\frac{\tau}{\tau_D}\right)^{-1}\left(1+\frac{\tau}{\omega^2\tau_D}\right)^{-1/2}\left(1+A\cdot\exp\left(-\frac{\tau}{\tau_R}\right)\right) \quad (2)$$

Eqn (1) is applied when fluorescence fluctuations arise only because of diffusion, and eqn (2) is applied when some other processes influence the fluorescence intensity fluctuations in the observation volume in addition to diffusion. In the above equations, τ_D is the time constant for diffusion, N is the number of particles in the observation volume, $\omega = l/r$ is the ratio of the longitudinal to transverse radius of the 3D Gaussian volume, A is the amplitude of processes other than diffusion that may give rise to fluorescence fluctuations, and τ_R is the timescale of such processes. We get two parameters, τ_D and τ_R, *via* fitting the fluorescence intensity auto-correlation curve. From the diffusion time (τ_D) and transverse radius of the observation volume (r), the diffusion coefficient (D_t) and hydrodynamic radius (r_H) of a diffusing particle can be calculated using the following equations:[76]

$$D_t = \frac{r^2}{4\tau_D} \quad (3)$$

$$r_H = \frac{k_B T}{6\pi\eta D_t} \quad (4)$$

where k_B is the Boltzmann constant, T is the temperature in Kelvin, and η is the viscosity of the medium. We measured several fluorescence intensity autocorrelation curves of rhodamine 6G (R6G) at varying concentrations in water and fitted them globally to determine the value of ω. While calibrating the value of ω, the diffusion coefficient of R6G in water is taken to be $D_t = 4.14 \times 10^{-6}$ cm^2 s^{-1}.[77] For a particular set of experiments, while fitting the data with eqn (1) and (2), ω is kept fixed.

In the presence of external additives, the refractive index and viscosity of a solution may change significantly in addition to the diffusion. We have rectified the effects of viscosity changes *via* performing control experiments at every experimental point, taking R6G as the fluorophore. R6G is a rigid molecule and will not undergo any structural changes when exposed to a DES at various degrees of hydration. In this way, any changes in its diffusion time through the detection volume will be solely because of differences in the medium viscosity. Using this information and the reported value of the hydrodynamic radius of R6G (7.7 Å) in pH 7.4 buffer, we can calculate the hydrodynamic radius of bromelain at every experimental point according to the following equation:

$$r_H = r_H^{R6G} \times \frac{\tau_D}{\tau_D^{R6G}} \quad (5)$$

The refractive index change is compensated for *via* changing the objective collar position and setting it to have the highest $G(0)$ value for each of the samples. In this way, we maintain the lowest detection volume attainable for each sample.

2.6. Activity measurements

The bromelain activity is assayed *via* a spectrophotometric method using casein as the substrate.[47,51,53] For activity measurements, untagged bromelain is used. Casein (0.3 mL, 1.5% w/v) was denatured at 70 °C for 15 min and was treated with bromelain (0.3 mL, 0.12 mg mL^{-1}) in 50 mM pH 7.4 phosphate buffer at 37 °C for 10 min. The reaction was then stopped *via* the addition of 0.3 mL of 200 mM trichloroacetic acid. The precipitate was removed through centrifugation, and the absorbance of the supernatant was measured at 280 nm. The value of the absorbance at 280 nm is proportional to the degree of the proteolysis of bromelain. Thus, we represent the activity of bromelain as the absorbance value obtained from 10 min of digestion. An appropriate blank value (consisting of all the constituents except bromelain) is subtracted from every measurement.

3. Results and discussion

3.1. Fluorescent tagging

Bromelain has five cysteine amino acid residues; of these, two pairs are connected by disulfide linkages, and the remaining one (Cys-25) is present in free/reactive form (Fig. 1). More interestingly, this Cys-25 residue is present at the active site of bromelain.[78]

This residue was tagged with 7-diethylamino-3-(4-maleimidophenyl)-4-methylcoumarin (CPM) and tetramethylrhodamine-5-maleimide (TMR) (Fig. 2a and c). CPM is weakly fluorescent in water with an emission maximum at 482 nm. Upon tagging, it becomes highly fluorescent, probably because of the restricted rotation of the 7-diethylamino moiety inside the protein matrix, and the emission maximum is blue-shifted to 475 nm (Fig. 2b). Such a blue shift of the emission maximum might be ascribed to the embedding of CPM inside the hydrophobic protein core of bromelain, thus confirming the tagging. TMR is not a solvatochromic dye, and there are no changes in its emission behaviour upon tagging Cys-25 of bromelain (Fig. 2d). The absorption profiles of CPM and TMR do not change upon tagging bromelain

(see Fig. S1 of the ESI†). The tagging is confirmed *via* measuring the diffusion time of the dye through a certain volume using FCS. The diffusion times of free CPM and CPM-tagged bromelain are found to be 22 and 67 μs, respectively, through an observation volume of 0.5 fL (Fig. 2e). For free TMR and TMR-tagged bromelain, the diffusion times through an observation volume of 0.7 fL are respectively measured to be 31 and 94 μs (Fig. 2f). Such an increase in the diffusion coefficient also proves the success of tagging. Furthermore, taking advantage of the solvatochromism of CPM, CPM fluorescence might be used to obtain information about local conformational alterations around Cys-25. The local conformation around the tagging site has been contemplated based on CPM emission for other proteins, like human serum albumin and β-lactoglobulin.[60,76] However, to do this, one needs to confirm that tagging has not perturbed the protein structure. We compared the CD spectra of untagged bromelain, CPM-tagged bromelain, and TMR-tagged bromelain, as seen in Fig. 2g. The almost similar CD spectra (secondary structural parameters are given in Table S1 of the ESI†) prove that tagging has not significantly perturbed the structural features of bromelain. The spectroscopic signals of CPM-bromelain and TMR-bromelain remain unaltered, even after 3 months.

3.2. Steady-state absorption and emission studies

As discussed above, changes in the microenvironment around the active site of bromelain can be monitored through steady-state absorption and emission studies of CPM as it is tagged to the Cys-25 residue of bromelain. To investigate the effects of the 0.5Ac/0.3Ur/0.2Sor DES on this, we recorded the absorption and emission spectra of CPM-tagged bromelain in the presence of varying amounts of DES (0% to 80% V/V) in phosphate buffer. The absorption spectra of CPM tagged to bromelain do not change in the presence of DES (data not shown). In the presence of 0–30% V/V DES, a small redshift in the emission spectrum was observed (λ_{em}^{max} = 478.5 nm in the presence of 30% V/V DES) with a slight decrease in the emission intensity (Fig. 3a and b). Upon a further increase in the DES content, the emission maximum was gradually blue-shifted and reached 471.5 nm at 80% V/V DES. The result suggests that at a lower DES content, CPM at the active site of bromelain experiences a hydrophilic environment, and as the DES content increases, the environment near the active site becomes more hydrophobic. However, reaching such a conclusion only from steady-state experiments is premature. As the surface accessibility of Cys-25 of bromelain is around 95%,[79] we believe that the steady-state emission characteristics of CPM tagged to Cys-25 of bromelain are mainly controlled by the external solvent medium rather than the protein matrix. Basically, with increasing DES content, the polarity of the solvent might change, and it is possible that the trend of the emission maximum of CPM at the active site of bromelain follows the bulk solvent polarity. To examine this possibility, we estimated the polarity of the 0.5Ac/0.3Ur/0.2Sor DES with various degrees of hydration through steady-state emission studies, using coumarin 1 (C1) as the solvatochromic dye (see Fig. 3c and Table 1). C1 is analogous with CPM and experiences a large change in dipole moment upon photoexcitation, which makes it an excellent solvatochromic probe.[80] As suspected, the trend is found to be similar to that of CPM tagged to the active site of bromelain. We thus conclude that the steady-state measurements are inconclusive.

3.3. CD studies

CD measurements would be useful for deciphering the modulations of the secondary structural parameters of bromelain in the presence of the DES. However, we could not perform CD measurements in the presence of the DES, as the DES has considerable absorption below 240 nm. Therefore, we could not directly comment on the modulation of the secondary structure of bromelain in the DES. However, we back-extracted bromelain from the DES and recorded CD spectra. If the DES modulates the secondary structure of bromelain irreversibly, this will be imprinted in the CD signal. The results are shown in Fig. S2 and Table S2 of the ESI.† It is clear that back-extracted bromelain from the DES retains most of its secondary structure. Therefore, we may conclude that the DES does not modify the secondary structure of bromelain irreversibly.

3.4. FCS studies

The fluorescence intensity autocorrelation curves of both CPM- and TMR-tagged bromelain could be best fitted using eqn (2)

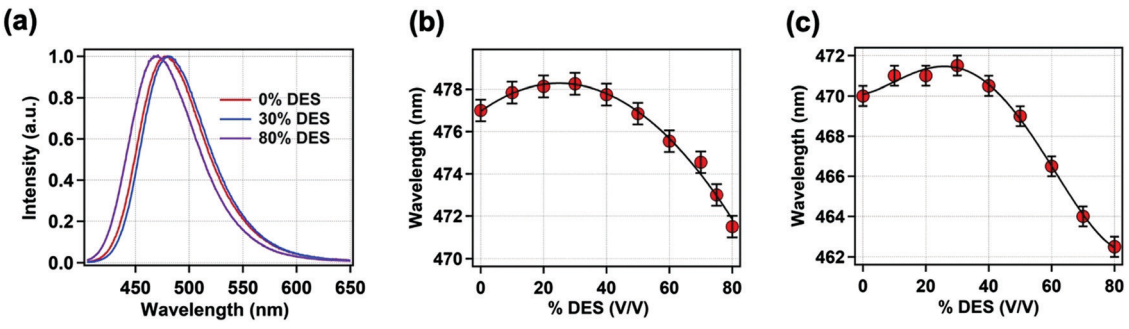

Fig. 3 Steady-state emission studies. (a) Representative emission spectra of CPM tagged to bromelain at various DES content levels. (b) The variation of the emission maximum of CPM tagged to bromelain with increasing DES concentration. (c) The variation of the emission maximum of coumarin-1 with increasing DES concentration. The black lines are guides for the eye, every experimental point is the average value of three independent measurements, and the error bars represent standard deviations of the mean values.

Table 1 Various properties of bromelain and the solvent medium as a function of the 0.5Ac/0.3Ur/0.2Sor DES content

DES content (%, V/V)	Emission maximum of coumarin-1 (nm)	Hydrodynamic radius of bromelain (Å)	Conformational fluctuation time of bromelain (μs)	Activity of bromelain	Viscosity of solvent measured *via* FCS (cP)
0	470.0	22.0	7.2	0.136	1.0
10	471.0	22.4	6.9	0.142	1.1
20	471.0	21.1	7.1	0.162	1.9
30	471.5	18.2	7.4	0.171	3.3
40	470.5	19.9	9.0	0.156	3.7
50	469.0	27.0	11.5	0.141	6.5
60	466.5	30.0	13.4	0.123	9.4
70	464.0	32.1	14.1	0.123	22.3
80	462.5	32.3	15.3	0.103	41.6

(see Fig. S3 of the ESI†), returning two time-related components. The exponential time component of 7 μs is assigned as the conformational fluctuation time of the active site of bromelain. Further, we performed the following control experiments to confirm this as the timescale of the conformational dynamics. (i) Although CPM is a weakly fluorescent molecule, it is possible to obtain the FCS data for CPM only. The data can be fitted (from 1 μs) using eqn (1) quite satisfactorily. TMR is substituted rhodamine, which is known to have a triplet-state blinking timescale of around 1 μs. The autocorrelation trace of TMR is not correctly fitted using eqn (1) from 1 μs. However, the fitting quality is quite good when fitted from 5 μs, implying that the effects of the dye photophysics die off beyond 5 μs. However, neither the CPM-tagged bromelain (from 1 μs) nor TMR-tagged bromelain (from 5 μs) autocorrelation curve can be fitted with eqn (1) (Fig. S1, ESI†). Therefore, the requirement for an additional relaxation term implies that the origin of the term arises not from the photophysics of the dye but from protein conformational fluctuations. (ii) Power-dependent experiments can also be beneficial when investigating the origin of the extra relaxation term. If the term originates from triplet-state blinking, the contribution should be affected by the power of the laser. However, that is not the case (see Fig. S4 of the ESI†). (iii) The exponential time component is also similar when employing two different tags (CPM and TMR). These aspects further confirm that the additional time component of 7 μs is the timescale of the bromelain conformational dynamics. The longer time component, τ_D, can be converted to a hydrodynamic radius, as described in the experimental section. The hydrodynamic radius is calculated to be 21 Å for both CPM- and TMR-tagged bromelain, which is in accordance with a previously measured hydrodynamic radius value of 23 Å *via* dynamic light scattering (DLS).[81] We have used the FCS data of TMR-tagged bromelain with increasing DES concentration (see Fig. 4a) instead of CPM.[82]

Upon increasing the DES content, we observe a slight decrease in the hydrodynamic radius up to 30% (V/V) DES, and with the further addition of the DES, the hydrodynamic radius gradually increases and reaches 32 Å at 80% DES (Fig. 4b and Table 1). The results suggest that bromelain adopts a slightly compact configuration in the presence of a small amount of the DES. However, with a further increase in the DES content, the interactions that held the tertiary structure together gradually break down, and bromelain adopts an

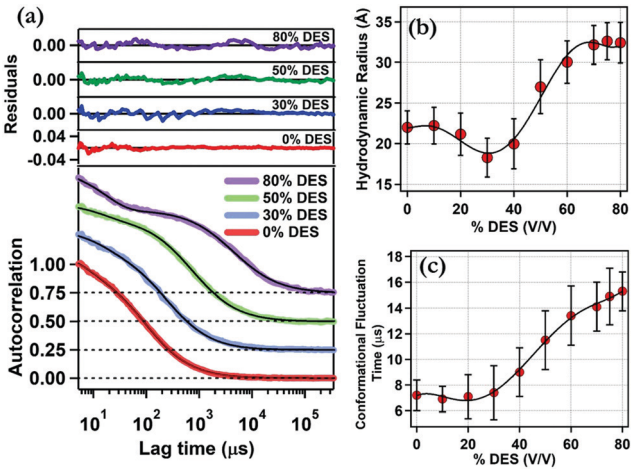

Fig. 4 Single-molecule-level FCS measurements of TMR tagged to bromelain. (a) Normalized fluorescence intensity autocorrelation curves for TMR-tagged bromelain at representative DES concentrations. Fitting lines based on eqn (2) are shown with solid black lines. The residuals of fitting are also shown in the upper panel. (b) Variations of the hydrodynamic radius of TMR-tagged bromelain with increasing DES concentration. (c) Variations of the conformational fluctuation time of TMR-tagged bromelain with increasing DES concentration. The black lines here are guides for the eye. Every experimental data point is the average of three independent measurements, and the error bars indicate standard deviations of mean values.

elongated/denatured conformation. Note that the emission study apparently contradicts these FCS results. However, the emission study gives information about the very local environment of the dye, and FCS furnishes information about the global protein structure. Moreover, we have already proved that the change in the emission maximum of CPM tagged to bromelain in the DES with various degrees of hydration is mainly due to changes in the solvent properties, not the protein properties.

Upon increasing the DES content, the conformational fluctuation time of bromelain gradually increases (more prominently beyond 30% (V/V) DES), suggesting the increased rigidness of the active site of bromelain (Fig. 4c and Table 1). The rigidity of the protein matrix might be modulated based on structural modulation, and with the opening of bromelain, such rigidity should decrease. Moreover, the dye tagged to Cys-25 of bromelain is at the protein surface and is mostly exposed to the solvent. Therefore, solvent viscosity should also play a crucial role in controlling the timescale of such motion.

3.5. Activity measurements

We studied the protease activity of bromelain with casein as a substrate in the 0.5Ac/0.3Ur/0.2Sor DES at various hydration levels. In buffer, the absorbance of digested casein is 0.136. At a low DES content, the activity increases slightly and reaches 0.171 at 30% (V/V) DES. However, with a further increase in the DES content, the activity drops and become 0.103 at 80% (V/V) DES (Fig. 5 and Table 1). It is interesting to note that even in the presence of 80% (V/V) DES, bromelain retains most of its activity. Moreover, at 30% (V/V) DES, the proteolytic activity of bromelain is found to be higher compared to that in buffer medium. As a control experiment, we performed activity measurements in a solution of the DES constituents, maintaining the same component concentrations as in hydrated DES. We cannot perform this experiment beyond 60% DES components in buffer because of solubility issues. Here, at 30% (v/v) DES components, the activity is measured to be 0.148.

3.6. Correlating the activity of bromelain with its structure/dynamics and DES properties

We attempted to find the correlations between the activity of bromelain and its structure and dynamics in the 0.5Ac/0.3Ur/0.2Sor DES at various degrees of hydration (Fig. 6). Up to 30% v/v DES in buffer enhances the activity of bromelain, followed by a decrease in activity as the fraction of DES increases. This report is in line with several previous experimental reports in which enzymes showed increased catalytic activities at higher water content levels and decreased activities at higher DES content levels.[33,39,83–85] However, a comprehensive explanation is difficult in this case, as mutual interplay between various factors and the enormous complexity of biomolecules place restrictions on drawing general rules. The structure is one of the main factors determining function. From FCS measurements, we observed that the native structure of bromelain is destroyed at increased concentrations of the DES and the activity decreased. However, at low DES content, bromelain becomes more compact and shows greater activity than in its native state. The second factor that controls the activity of a protein is its dynamics. In particular, the μs dynamics of the active site are believed to be a controlling factor for enzymatic activity. We have seen that with an increase in DES concentration, the timescale of the conformational fluctuation dynamics of bromelain increases. This suggests that bromelain becomes more and more rigid with an increase in DES content. Probably, the decreased flexibility plays a role in reducing the activity of bromelain at higher DES content levels. Overall, we see fascinating correlation between structure, active-site dynamics, and bromelain activity, *i.e.*, (i) structural compaction and flexibility favour the activity and (ii) structural elongation and rigidity lead to less activity (see Fig. 6).

Next, we tried to gain an understanding of how the activity of bromelain is modulated based on the DES properties due to different extents of hydration. The change in the emission maximum of coumarin-1 (a positive solvatochromic dye) in the 0.5Ac/0.3Ur/0.2Sor DES with various degrees of hydration can be ascribed to a change in the polarity of the DES at different degrees of hydration. Here, a redshift in the emission maximum indicates increased solvent polarity. Interestingly, we get excellent correlation between polarity and activity (Fig. 6). At 30% (V/V) DES and 80% (V/V) DES, the polarity is at its maximum and minimum, respectively, and so is the bromelain activity. Both the enzyme and the substrate, in this case, are large biomolecules. Therefore, diffusion must have a prominent role to play in controlling the proteolytic activity. Diffusion is dictated by the friction experienced by bromelain or casein while moving in the medium and is greatly governed by the medium viscosity. The viscosity of the medium has been estimated based on the diffusion time of R6G (see Fig. S5 of the ESI† and Table 1). Upon increasing the DES content, the viscosity gradually increases and diffusion becomes progressively slower. As per our predictions, the activity of bromelain should decrease gradually with an increase in the DES content and, in fact, at high DES content levels, we found an activity decrease (Fig. 6). However, the initial increase in activity cannot be rationalised through viscosity changes, and we believe that this is mostly controlled by the structure. Most probably, the overall result is a combined effect of all possible causes. Overall, we propose that a solvent that can compact the bromelain structure and increase its flexibility might be a better medium

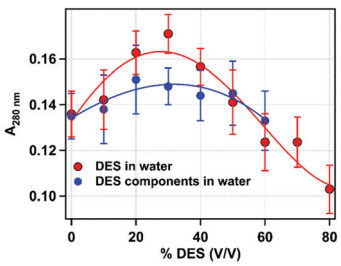

Fig. 5 Variations in the activity of untagged bromelain with increasing 0.5Ac/0.3Ur/0.2Sor DES concentration (red) and the activity in a solution of the DES constituents (blue), maintaining the same component concentration as in hydrated DES. We cannot perform this experiment beyond 60% for the DES components in buffer because of solubility issues. The solid lines are guides for the eye. Every experimental data point is the average of three independent measurements, and the error bars indicate standard deviations of the mean values.

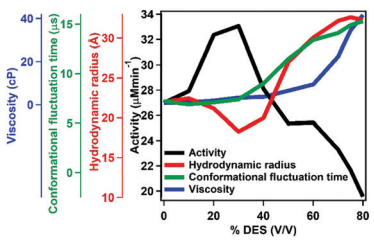

Fig. 6 Correlating the activity of bromelain with its structure and active-site dynamics and the viscosity of the medium with increasing DES concentration. Structural compaction, decreased active-site conformational fluctuation time, and low viscosity favour the activity of bromelain. In contrast, an elongated structural conformation, increased conformational fluctuation time, and increased medium viscosity disfavour the activity of bromelain.

for increasing its activity based on such correlation. Further, it is probable that a solvent with low viscosity and high polarity is a better choice.

One may argue that dilution with water might lead to the disruption of the DES network. Therefore, it is hard to tell if the noted positive effects of the DES in the low-concentration region are due to the nature of the DES, *i.e.*, the hydrogen-bonded solvent network, or due to normal salting-in effects. Previous studies have shown that for many DESs, the network is maintained up to a certain water concentration.[86–91] For example, in the case of a choline–chloride/urea DES, the network is found to be maintained up to ~83 mol% water.[86] If that is the case, then at high water content levels, the interactions of individual DES components with water and the protein will mainly control the protein behaviour rather than the network-like DES nature. To gain more insight into this, we have done a control experiment. We mixed all three constituents of DES in water, maintaining the same component concentrations as in hydrated DES, and recorded the proteolytic activity of bromelain (see Fig. 5). Here, we observed a definitive but slight increase in the proteolytic activity compared to pure buffer at higher water concentrations, in contrast to the significant effect arising from the corresponding DES. Therefore, there is a hint that synergistic action from the individual components might play a role. Nevertheless, the noted positive effects on bromelain activity in the hydrated DES probably arise due to the nature of the DES itself, *i.e.*, a hydrogen-bonded solvent network. Earlier, increases in peroxidase[33] and lipase[92] activities were proposed not to arise solely due to a synergistic effect, even at higher degrees of dilution. In the present case we also propose that even at high water content levels, the DES still exists as a somewhat intact entity. However, the properties of the DES itself would need to be studied to confirm this proposition, and neutron scattering might come in handy.

4. Summary and conclusions

In conclusion, we examined the behaviour of bromelain, an industrially important proteolytic enzyme, in a hydrated DES composed of acetamide, urea, and sorbitol (0.5Ac/0.3Ur/0.2Sor). Moreover, we tried to correlate the proteolytic behaviour with the protein structure and dynamics and with the various properties of the DES. The main findings can be summarised as follows. (i) The structure becomes slightly more compact at a lower DES concentration (30% V/V) but it becomes elongated at higher DES concentrations. (ii) The microsecond protein dynamics become progressively slower with increasing DES concentration. (iii) The enzymatic activity of bromelain is retained in the DES. More importantly, at some DES concentrations, the activity is even higher than in the native state. (iv) We find interesting correlation between the activity of bromelain and its structure and dynamics and the DES properties. We conclude that a more compact structural conformation, higher active-site flexibility, low solvent medium viscosity, and greater polarity probably facilitate protein function. (v) The noted positive effects of the DES on the activity of bromelain under highly diluted conditions are probably due to the effects of the network-like DES structure.

Overall, our results provide deeper insight regarding the correlation between the structure, activity, and dynamics of bromelain in the 0.5Ac/0.3Ur/0.2Sor DES. We also investigated the correlation between the activity of bromelain and the DES properties (*i.e.*, the extent of hydration, viscosity, and polarity). We believe that such insights will be beneficial for the rational design of DESs as biocatalytic media. However, keeping in mind the enormous complexity of biological systems, it is very tough to prescribe how enzymatic activities can be optimized. Huge effort is necessary in this regard.

Author contributions

Nilimesh Das: conceptualization, methodology, investigation, formal analysis, writing – original draft, writing – review and editing. Tanmoy Khan: investigation, formal analysis, writing – original draft. Navin Subba: investigation. Pratik Sen: conceptualization, project administration, resources, funding acquisition, supervision, validation, writing – review and editing.

Conflicts of interest

The authors declare no competing financial interests.

Acknowledgements

ND, TK, and NS thank the Council of Scientific and Industrial Research, Prime Minister Research Fellowship and Indian Institute of Technology Kanpur, respectively, for providing graduate fellowships. PS thanks Indian Institute of Technology Kanpur for infrastructure and support. This work is financially supported by the Science and Engineering Research Board, Government of India (Grant No. EMR/2016/006555).

References

1 M. O. Simon and C. J. Li, *Chem. Soc. Rev.*, 2012, **41**, 1415–1427.
2 M. Raj and V. K. Singh, *Chem. Commun.*, 2009, 6687–6703.
3 M. Gruttadauria, F. Giacalone and R. Noto, *Adv. Synth. Catal.*, 2009, **351**, 33–57.
4 M. P. van Der Helm, B. Klemm and R. Eelkema, *Nat. Rev. Chem.*, 2019, **3**, 491–508.
5 M. D. Hoang, R. A. Kumar, D. A. Buisson, W. L. Ling, E. Gravel and E. Doris, *ChemCatChem*, 2020, **12**, 1156–1160.
6 M. L. Contente, A. Pinto, F. Molinari and F. Paradisi, *Adv. Synth. Catal.*, 2018, **360**, 4814–4819.
7 D. H. Nam, G. M. Ryu, S. K. Kuk, E. J. Son and C. B. Park, *Appl. Catal.*, 2016, **198**, 311–317.
8 B. Grabner, A. K. Schweiger, K. Gavric, R. Kourist and H. Gruber-Woelfler, *React. Chem. Eng.*, 2020, **5**, 263–269.

9 E. Calla-Quispe, J. Robles, C. Areche and B. Sepulveda, *Front. Chem.*, 2020, **8**, 450.
10 D. C. Murador, L. M. de Souza Mesquita, N. Vannuchi, A. R. C. Braga and V. V. de Rosso, *Curr. Opin. Food Sci.*, 2019, **26**, 25–34.
11 Y. Liu, X. Chen, S. Men, P. Licence, F. Xi, Z. Ren and W. Zhu, *Phys. Chem. Chem. Phys.*, 2019, **21**, 11058–11065.
12 J. E. Bara, A. Finotello, J. W. Magee, S. Qian, K. E. O'Harra, G. P. Dennis and R. D. Noble, *Ind. Eng. Chem. Res.*, 2019, **58**, 17956–17964.
13 P. D. de María and Z. Maugeri, *Curr. Opin. Chem. Biol.*, 2011, **15**, 220–225.
14 J. Gorke, F. Srienc and R. Kazlauskas, *Biotechnol. Bioprocess Eng.*, 2010, **15**, 40–53.
15 F. S. Mjalli and O. U. Ahmed, *Asia-Pac. J. Chem. Eng.*, 2016, **11**, 549–557.
16 W. Guo, Y. Hou, S. Ren, S. Tian and W. Wu, *J. Chem. Eng. Data*, 2013, **58**, 866–872.
17 M. Hayyan, Y. P. Mbous, C. Y. Looi, W. F. Wong, A. Hayyan, Z. Salleh and O. Mohd-Ali, *SpringerPlus*, 2016, **5**, 913.
18 H. Vanda, Y. Dai, E. G. Wilson, R. Verpoorte and Y. H. Choi, Green solvents from ionic liquids and deep eutectic solvents to natural deep eutectic solvents, *C. R. Chim.*, 2018, **21**, 628–638.
19 B. Kudłak, K. Owczarek and J. Namieśnik, *Environ. Sci. Pollut. Res.*, 2015, **22**, 11975–11992.
20 F. Janati-Fard, M. R. Housaindokht, H. Monhemi, A. A. Esmaeili and A. N. Pour, *Int. J. Biol. Macromol.*, 2018, **114**, 656–665.
21 F. van Rantwijk, F. Secundo and R. A. Sheldon, *Green Chem.*, 2006, **27**, 282–286.
22 N. Yadav, K. Bhakuni, M. Bisht, I. Bahadur and P. Venkatesu, *ACS Sustainable Chem. Eng.*, 2020, **27**, 10151–10160.
23 A. Sanchez-Fernandez, K. J. Edler, T. Arnold, D. A. Venero and A. J. Jackson, *Phys. Chem. Chem. Phys.*, 2017, **19**, 8667–8670.
24 S. M. Andler, L. S. Wang, V. M. Rotello and J. M. Goddard, *J. Agric. Food Chem.*, 2017, **65**, 1907–1914.
25 J. A. Kist, M. T. Henzl, J. L. Bañuelos and G. A. Baker, *ACS Sustainable Chem. Eng.*, 2019, **7**, 12682–12687.
26 P. Pradeepkumar, N. K. Rajendran, A. A. Alarfaj, M. A. Munusamy and M. Rajan, *ACS Appl. Bio Mater.*, 2018, **1**, 2094–2109.
27 S. L. Cao, H. Xu, X. H. Li, W. Y. Lou and M. H. Zong, *ACS Sustainable Chem. Eng.*, 2015, **3**, 1589–1599.
28 R. Esquembre, J. M. Sanz, J. G. Wall, F. del Monte, C. R. Mateo and M. L. Ferrer, *Phys. Chem. Chem. Phys.*, 2013, **15**, 11248–11256.
29 A. Sindhu, S. Kumar, D. Mondal, I. Bahadur and P. Venkatesu, *Phys. Chem. Chem. Phys.*, 2020, **22**, 14811–14821.
30 H. Monhemi, M. R. Housaindokht, A. A. Moosavi-Movahedi and M. Reza-Bozorgmehr, *Phys. Chem. Chem. Phys.*, 2014, **16**, 14882–14893.
31 C. Zhao, J. Ren and X. Qu, *Langmuir*, 2013, **29**, 1183–1191.
32 M. L. Toledo, M. M. Pereira, M. G. Freire, J. P. A. Silva, J. A. P. Coutinho and A. P. M. Tavares, *ACS Sustainable Chem. Eng.*, 2019, **7**, 11806–11814.
33 A. A. Papadopoulou, E. Efstathiadou, M. Patila, A. C. Polydera and H. Stamatis, *Ind. Eng. Chem. Res.*, 2016, **55**, 5145–5151.
34 W. Qu, R. Häkkinen, J. Allen, C. D'Agostino and A. P. Abbott, *Molecules*, 2019, **24**, 3583.
35 B. Olivares, F. Martínez, L. Rivas, C. Calderón, J. M. Munita and P. R. Campodonico, *Sci. Rep.*, 2018, **8**, 1–12.
36 A. A. Elgharbawy, A. Hayyan, M. Hayyan, S. N. Rashid, M. R. M. M. Y. Zulkifli, Y. Alias and M. E. S. Mirghani, *Chem. Biochem. Eng. Q.*, 2018, **32**, 359–370.
37 Y. Dai, J. van Spronsen, G. J. Witkamp, R. Verpoorte and Y. H. Choi, *Anal. Chim. Acta*, 2013, **766**, 61–68.
38 A. Gertrudes, R. Craveiro, Z. Eltayari, R. L. Reis, A. Paiva and R. C. Duarte, *ACS Sustainable Chem. Eng.*, 2017, **5**, 9542–9553.
39 Y. H. Choi, J. van Spronsen, Y. Dai, M. Verberne, F. Hollmann, I. W. Arends, G. J. Witkamp and R. Verpoorte, *Plant Physiol.*, 2011, **156**, 1701–1705.
40 R. Cavicchioli, T. Charlton, H. Ertan, S. M. Omar, K. S. Siddiqui and T. J. Williams, *Microb. Biotechnol.*, 2011, **4**, 449–460.
41 O. Kirk, T. V. Borchert and C. C. Fuglsang, *Curr. Opin. Biotechnol.*, 2002, **13**, 345–351.
42 I. Alkorta, C. Garbisu, M. J. Llama and J. L. Serra, *Biochemistry*, 1998, **33**, 21–28.
43 B. López-García, M. Hernández and B. S. Segundo, *Lett. Appl. Microbiol.*, 2012, **55**, 62–67.
44 R. Pavan, S. Jain and A. Kumar, *Biotechnol. Res. Int.*, 2012, **2012**, 976203.
45 B. Seligman, *Angiology*, 1962, **13**, 508–510.
46 C. Metzig, E. Grabowska, K. Eckert, K. Rehse and H. R. Maurer, *In Vivo*, 1999, **13**, 7–12.
47 A. Rani and P. Venkatesu, *Int. J. Biol. Macromol.*, 2015, **73**, 189–201.
48 I. Jha, M. Bisht and P. Venkatesu, *J. Phys. Chem. B*, 2016, **120**, 5625–5633.
49 I. Jha, M. Bisht, N. K. Mogha and P. Venkatesu, *J. Phys. Chem. B*, 2018, **122**, 7522–7529.
50 S. Habib, M. A. Khan and H. Younus, *Protein J.*, 2007, **26**, 117–124.
51 A. Rani and P. Venkatesu, *J. Phys. Chem. B*, 2016, **120**, 8863–8872.
52 A. Rani, M. Taha, P. Venkatesu and M.-J. Lee, *J. Phys. Chem. B*, 2017, **121**, 6456–6470.
53 K. Bhakuni and P. Venkatesu, *Int. J. Biol. Macromol.*, 2019, **131**, 527–535.
54 P. Kiran, I. Jha, A. Sindhu, P. Venkatesu, I. Bahadur and E. E. Ebenso, *J. Mol. Liq.*, 2020, **297**, 111785.
55 P. K. Kumar, M. Bisht, P. Venkatesu, I. Bahadur and E. E. Ebenso, *J. Phys. Chem. B*, 2018, **122**, 10435–10444.
56 P. K. Kumar, I. Jha, P. Venkatesu, I. Bahadur and E. E. Ebenso, *J. Mol. Liq.*, 2017, **246**, 178–186.
57 N. K. Mogha, A. Sindhu and P. Venkatesu, *Int. J. Biol. Macromol.*, 2020, **151**, 957–966.
58 J. Guo and H. X. Zhou, *Chem. Rev.*, 2016, **116**, 6503–6515.
59 J. M. Yon, D. Perahia and C. Ghelis, *Biochimie*, 1998, **80**, 33–42.

60 D. K. Sasmal, T. Mondal, S. S. Mojumdar, A. Choudhury, R. Banerjee and K. Bhattacharyya, *J. Phys. Chem. B*, 2011, **115**, 13075–13083.
61 S. S. Mojumdar, R. Chowdhury, S. Chattoraj and K. Bhattacharyya, *J. Phys. Chem. B*, 2012, **116**, 12189–12198.
62 S. Ghosh, S. Parui, B. Janaand and K. Bhattacharyya, *J. Chem. Phys.*, 2015, **143**, 125103.
63 A. Pabbathi and A. Samanta, *J. Phys. Chem. B*, 2020, **124**, 8132–8140.
64 A. Pabbathi, S. Ghosh and A. Samanta, *J. Phys. Chem. B*, 2013, **117**, 16587–16593.
65 M. M. Islam, S. Barik, N. Preeyanka and M. Sarkar, *J. Phys. Chem. B*, 2020, **124**, 961–973.
66 M. M. Islam, S. Barik and M. Sarkar, *J. Phys. Chem. B*, 2019, **123**, 1512–1526.
67 N. Subba, P. Sahu, N. Das and P. Sen, *J. Chem. Sci.*, 2021, **133**, 25.
68 R. Yadav, B. Sengupta and P. Sen, *J. Phys. Chem. B*, 2014, **118**, 5428–5438.
69 B. Sengupta, N. Das and P. Sen, *Biochim. Biophys. Acta, Proteins Proteomics*, 2018, **1866**, 316–326.
70 T. Murachi, M. Yasui and Y. Yasuda, *Biochemistry*, 1963, **3**, 48–55.
71 G. Böhm, R. Muhr and R. Jaenicke, *Prot. Eng.*, 1992, **5**, 191–195.
72 B. Sengupta, N. Das and P. Sen, *Biophys. Chem.*, 2017, **221**, 17–25.
73 N. Das and P. Sen, *Biochemistry*, 2018, **57**, 6078–6089.
74 N. Das and P. Sen, *Int. J. Biol. Macromol.*, 2019, **141**, 843–854.
75 N. Das and P. Sen, *J. Phys. Chem. B*, 2020, **124**, 5858–5871.
76 J. R. Lakowicz, *Principles of Fluorescence Spectroscopy*, 3rd edn, Springer, New York, 2006.
77 C. B. Müller, A. Loman, V. Pacheco, F. Koberling, D. Willbold and W. J. Richtering, *Europhys. Lett.*, 2008, **83**, 46001.
78 S. S. Husain and G. Lowe, *Biochem. J.*, 1970, **117**, 341–346.
79 http://www.cbs.dtu.dk/services/NetSurfP.
80 N. Nemkovich, H. Reis and W. Baumann, *J. Lumin.*, 1997, **71**, 255–263.
81 M. Zaman, S. Zakariya, S. Nusrat, M. Khan, A. Qadeer, M. Ajmal and R. Khan, *J. Biomol. Struct. Dyn.*, 2017, **201**, 1407–1419.
82 Note: Steady-state fluorescence has been taken with CPM tagged bromelain because TMR is not a solvatochromic dye. In the case of FCS measurement, solvatochromism is not a necessary criterion. Moreover, Ac/Ur/Sor DES shows tiny emission around 450 nm when excited at 400 nm. This much emission is negligible compared to the emission from CPM molecule tagged to bromelain in the steady-state experiment when the concentration is around 5 μM. However, in the case of FCS, the sample concentration is in the nM range and therefore DES emission interfere with the fluorescence signal from the CPM tagged bromelain. As a result, we performed the FCS experiment with TMR tagged to bromelain.
83 E. Durand, J. Lecomte, B. Baréa and P. Villeneuve, *Eur. J. Lipid Sci. Technol.*, 2014, **116**, 16.
84 D. Lindberg, M. de la Fuente Revenga and M. J. Widersten, *J. Biotechnol.*, 2010, **147**, 169.
85 E. Durand, J. Lecomte, B. Baréa, E. Dubreucq, R. Lortie and P. Villeneuve, *Green Chem.*, 2013, **15**, 2275.
86 O. S. Hammond, D. T. Bowron and K. J. Edler, *Angew. Chem.*, 2017, **56**, 9782–9785.
87 S. Kaur, A. Gupta and H. K. Kashyap, *J. Phys. Chem. B*, 2020, **124**, 2230–2237.
88 S. Panda, K. Kundu, J. Kiefer, S. Umapathy and R. L. Gardas, *J. Phys. Chem. B*, 2019, **123**, 3359–3371.
89 L. Weng and M. Toner, *Phys. Chem. Chem. Phys.*, 2018, **20**, 22455–22462.
90 E. Posada, N. López-Salas, R. J. Riobóo, M. L. Ferrer, M. C. Gutiérrez and F. Del Monte, *Phys. Chem. Chem. Phys.*, 2017, **19**, 17103–17110.
91 R. Contreras, L. Lodeiro, N. Rozas-Castro and R. Ormazábal-Toledo, *Phys. Chem. Chem. Phys.*, 2021, **23**, 1994–2004.
92 Z. L. Huang, B. P. Wu, Q. Wen, T. X. Yang and Z. Yang, *J. Chem. Technol. Biotechnol.*, 2014, **89**, 1975–1981.

Electronic Supplementary Information

Correlating Bromelain's Activity with its Structure, Active-site Dynamics and Media's Physical Properties in a Hydrated Deep Eutectic Solvent

Nilimesh Das, Tanmoy Khan, Navin Subba and Pratik Sen*

Department of Chemistry, Indian Institute of Technology Kanpur, Kanpur – 208 016, UP, India

***Content*:**

Table S1. Secondary structural parameters of untagged, CPM tagged and TMR tagged bromelain.

	α-helicity	β-sheet	β-turn	Random Coil
Untagged Bromelain	20.1	22.4	18.0	39.5
CPM-Bromelain	19.6	22.4	17.5	40.5
TMR-Bromelain	20.0	22.3	18.0	39.7

Table S2. Secondary structural parameters of native bromelain and back extracted bromelain from various DES composition.

DES Content % (v/v)	α-helicity	β-sheet	β-turn	Random Coil
0	20.5	23.4	17.6	38.5
10	20.4	23.5	17.6	38.5
20	20.4	23.4	17.8	38.4
30	20.2	23.8	17.8	38.2
40	20.0	24.0	17.7	38.3
50	19.7	24.1	17.7	38.5
60	19.1	24.3	17.8	38.8
70	18.3	24.8	17.8	39.1
80	16.1	26.4	17.8	39.7

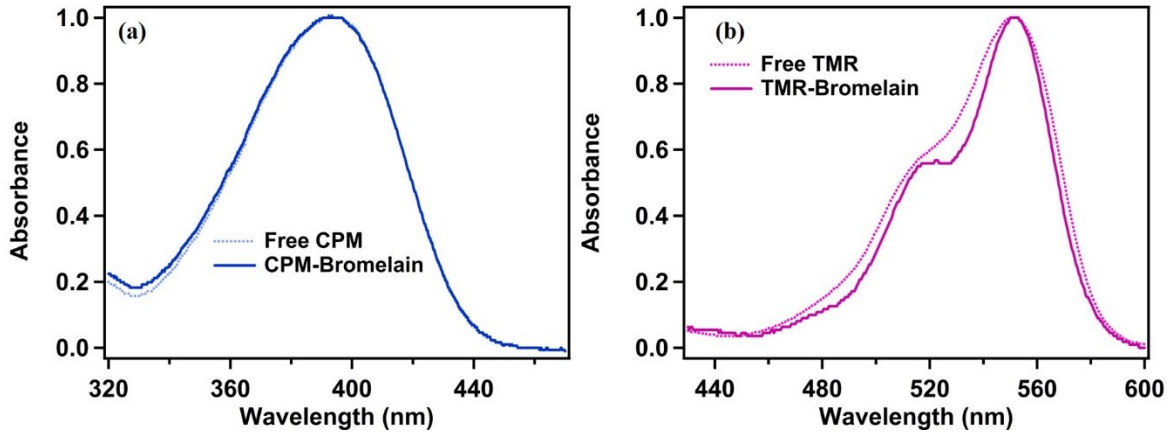

Figure S1. Absorption spectra of (a) free CPM and CPM tagged to bromelain; and (b) free TMR and TMR tagged to bromelain

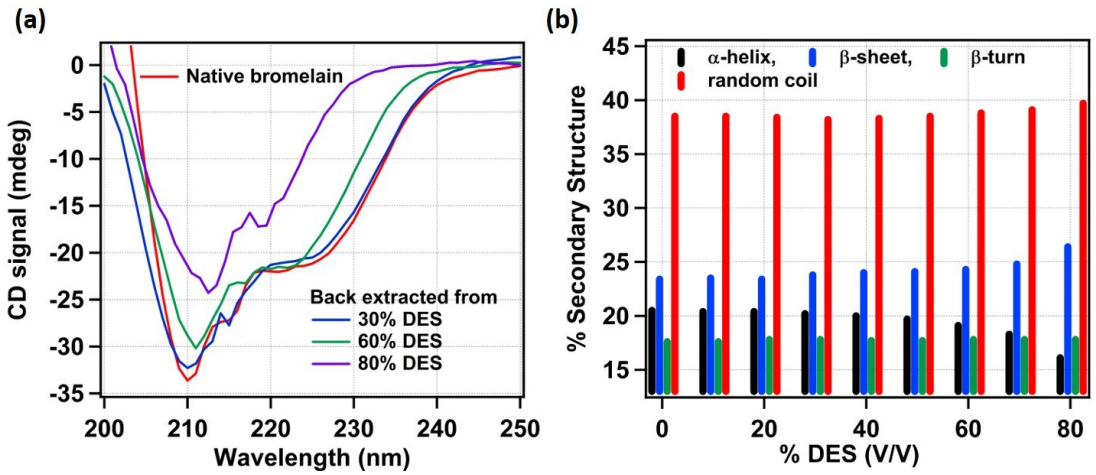

Figure S2. (a) CD spectra and (b) various secondary structural parameters of native bromelain in phosphate buffer (pH = 7.4) and back-extracted bromelain from various DES compositions. Bromelain concentration is 10 μM and path length is 2 mm.

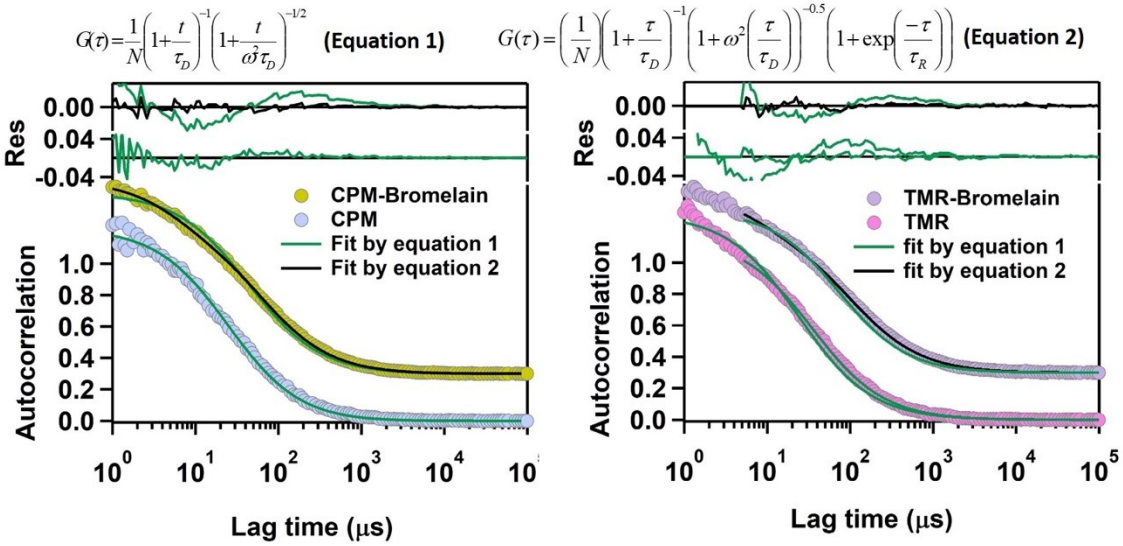

Figure S3. Fitting comparison of fluorescence autocorrelation traces of (a) CPM and CPM tagged to bromelain and (b) TMR and TMR tagged to bromelain. Equation 1 can fit the autocorrelation trace of CPM satisfactorily; but extra relaxation term is required to fit the autocorrelation trace of CPM-bromelain. Equation can fit the autocorrelation trace of TMR only when fitted from 5 μs. However, to fit autocorrelation trace of TMR-bromelain from 5 μs, equation 2 is required.

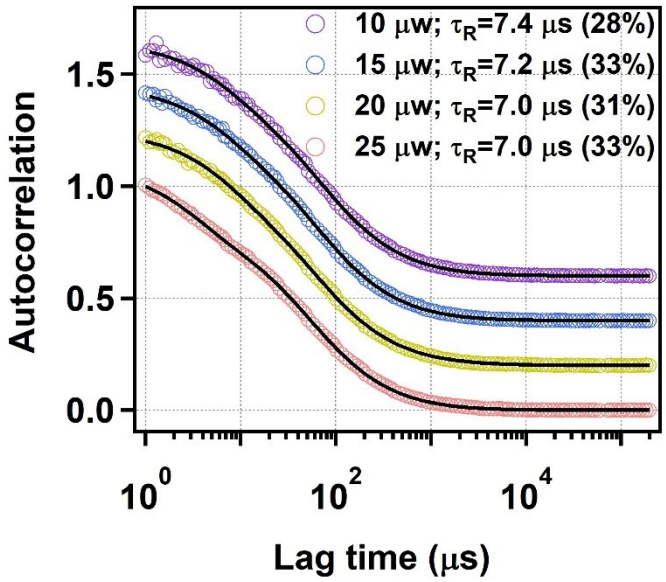

Figure S4. Autocorrelations traces of CPM tagged to bromelain at different laser power. The value of conformational fluctuation time and its contribution remains similar with the variation of power.

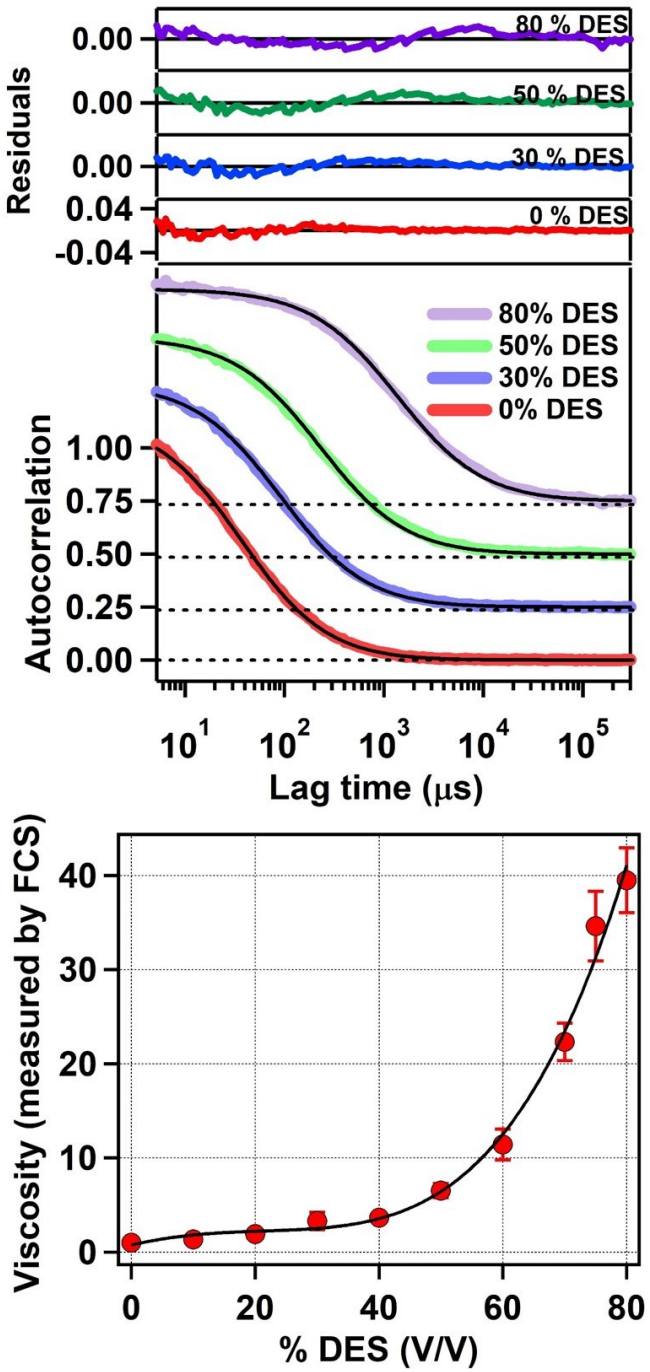

Figure S5. (a) Normalized fluorescence intensity autocorrelation curve for rhodamine-6G at some representative DES concentration. Fitting lines using equation 1 are shown by solid black lines. The residuals of fitting are also shown. (b) Variation of viscosity with increasing DES concentration